



The axial charge of the nucleon on the lattice and in chiral perturbation theory

Arifa Ali Khan^a, Meinulf Gockeler^{*a}, Philipp Hägler^b, Thomas R. Hemmert^b, Roger Horsley^c, Alan C. Irving^d, Dirk Pleiter^e, Paul E. L. Rakow^d, Andreas Schäfer^a, Gerrit Schierholz^{ef}, Hinnerk Stüben^g, Tim Wollenweber^b and James M. Zanotti^e

^a Institut für Theoretische Physik, Universität Regensburg, 93040 Regensburg, Germany

^b Physik-Department, Theoretische Physik, Technische Universität München, 85747 Garching, Germany

^c School of Physics, University of Edinburgh, Edinburgh EH9 3JZ, UK

^d Theoretical Physics Division, Department of Mathematical Sciences, University of Liverpool, Liverpool L69 3BX, UK

^e John von Neumann-Institut für Computing NIC, Deutsches Elektronen-Synchrotron DESY, 15738 Zeuthen, Germany

^f Deutsches Elektronen-Synchrotron DESY, 22603 Hamburg, Germany

^g Konrad-Zuse-Zentrum für Informationstechnik Berlin, 14195 Berlin, Germany

E-mail: meinulf.goeckeler@physik.uni-regensburg.de

QCDSF-UKQCD Collaboration

We present recent Monte Carlo data for the axial charge of the nucleon obtained by the QCDSF-UKQCD collaboration for $N_f = 2$ dynamical quarks. We compare them with formulae from chiral perturbation theory in finite and infinite volume and find a remarkably consistent picture.

XXIIIrd International Symposium on Lattice Field Theory

25-30 July 2005

Trinity College, Dublin, Ireland

*Speaker.

The QCDSF and UKQCD collaborations have generated ensembles of gauge field configurations using $N_f = 2$ non-perturbatively $O(a)$ improved Wilson quarks and Wilson's plaquette action for the gauge fields. Here we want to discuss the results obtained for the axial charge of the nucleon, g_A . Their interpretation is not straightforward because the quark masses in the simulations are larger than in nature, the volumes are somewhat smaller than infinity, the lattice spacings are larger than 0 etc. So we need some guidance for the extrapolations towards the physical quark masses, the thermodynamic and continuum limits. Such guidance is provided by chiral effective field theory (ChEFT), which for selected quantities, e.g. for g_A , yields parameterisations of the dependence on the quark mass and the volume which take into account the constraints imposed by (spontaneously broken) chiral symmetry. The dependence on the lattice spacing a can be included, but we shall not consider this possibility here. So we do not yet attempt to cope with the lattice artefacts remaining even after $O(a)$ improvement.

If ChEFT can be successfully applied, we gain control over the chiral extrapolation and the approach to the thermodynamic limit. At the same time we can determine not only the physical value of the quantity of interest, g_A in our case, but also some effective coupling constants. These may occur in the ChEFT expressions for other observables and be of phenomenological interest there. Establishing the link between Monte Carlo results and ChEFT will thus enable us to extract considerably more information from our simulations than just the physical value of the quantity under study.

In its standard form, ChEFT describes low-energy QCD by means of an effective field theory based on effective pion, nucleon, ... fields. Since the effective Lagrangian does not depend on the volume, besides the quark-mass dependence the very same Lagrangian governs also the volume dependence, and finite size effects can be calculated by evaluating the theory in a finite (spatial) volume. Thus the finite volume does not introduce any new parameters and the study of the finite size effects yields an additional handle on the coupling constants of ChEFT. The effective description will break down if the box length L becomes too small, just as it fails for pion masses that are too large.

The simulation parameters are listed in Table 1. Note that we have two groups of three ensembles each which differ only in the volume.

We compute g_A from forward proton matrix elements of the flavour-nonsinglet axial vector current $A_\mu^{u-d} = \bar{u}\gamma_\mu\gamma_5 u - \bar{d}\gamma_\mu\gamma_5 d$:

$$\langle p, s | A_\mu^{u-d} | p, s \rangle = 2g_A s_\mu. \quad (1)$$

The required bare matrix elements are extracted from ratios of 3-point functions over 2-point functions in the standard fashion. Compared to the computation of hadron masses, additional difficulties arise in the calculation of nucleon matrix elements such as g_A : In general there are quark-line disconnected contributions, which are hard to evaluate, the operators must be improved and renormalised etc. Fortunately, in the limit of exact isospin invariance, which is taken in our simulations, all disconnected contributions cancel in g_A , because it is a flavour-nonsinglet quantity. The improved axial vector current is given by

$$A_\mu^{\text{imp}}(x) = \bar{q}(x)\gamma_\mu\gamma_5 q(x) + ac_A \partial_\mu \bar{q}(x)\gamma_5 q(x), \quad (2)$$

Coll.	β	κ_{sea}	volume	Coll.	β	κ_{sea}	volume
QCDSF	5.20	0.1342	$16^3 \times 32$	UKQCD	5.29	0.1340	$16^3 \times 32$
UKQCD	5.20	0.1350	$16^3 \times 32$	QCDSF	5.29	0.1350	$16^3 \times 32$
UKQCD	5.20	0.1355	$16^3 \times 32$	QCDSF	5.29	0.1355	$12^3 \times 32$
QCDSF	5.25	0.1346	$16^3 \times 32$	QCDSF	5.29	0.1355	$16^3 \times 32$
UKQCD	5.25	0.1352	$16^3 \times 32$	QCDSF	5.29	0.1355	$24^3 \times 48$
QCDSF	5.25	0.13575	$24^3 \times 48$	QCDSF	5.29	0.1359	$12^3 \times 32$
QCDSF	5.40	0.1350	$24^3 \times 48$	QCDSF	5.29	0.1359	$16^3 \times 32$
QCDSF	5.40	0.1356	$24^3 \times 48$	QCDSF	5.29	0.1359	$24^3 \times 48$
QCDSF	5.40	0.1361	$24^3 \times 48$				

Table 1: Simulation parameters.

and hence the improvement term, i.e. the term proportional to c_A , does not contribute in forward matrix elements. The renormalised improved axial vector current can be written as

$$A_\mu = Z_A (1 + b_A am) A_\mu^{\text{imp}} \quad (3)$$

with the bare quark mass $m = (1/\kappa_{\text{sea}} - 1/\kappa_c)/(2a)$.

While the coefficient b_A will be computed in tadpole improved one-loop perturbation theory, we calculate the renormalisation factor Z_A non-perturbatively by means of the Rome-Southampton method [1, 2]. Thus Z_A is first obtained in the so-called RI'-MOM scheme. Using continuum perturbation theory we switch to the $\overline{\text{MS}}$ scheme. For sufficiently large renormalisation scales μ , Z_A should then be independent of μ . However, unless $\mu \ll 1/a$ lattice artefacts may spoil this behaviour. Since our scales do not always satisfy this criterion, we try to correct for this mismatch by subtracting the lattice artefacts perturbatively with the help of boosted one-loop lattice perturbation theory. Some lattice artefacts still remain, but we can nevertheless estimate Z_A . In Table 2 we compare our results with a recent determination of Z_A by the ALPHA collaboration [3].

β	5.20	5.25	5.29	5.40
this work	0.765(5)	0.769(4)	0.772(4)	0.783(4)
ALPHA	0.719	0.734	0.745	0.767

Table 2: Values of Z_A from this work and from the ALPHA collaboration.

Our results for g_A are plotted in Fig. 1. Here m_π has been taken from the largest available lattice at each $(\beta, \kappa_{\text{sea}})$ combination. The scale has been set by means of the force parameter r_0 with $r_0 = 0.467$ fm, and r_0/a has been taken at the given quark mass. Obviously there are considerable finite size effects. A similar volume dependence has already been observed in quenched simulations [4].

In order to describe or fit these data we use ChEFT. More specifically, we employ the so-called small scale expansion (SSE) [5], which is one possibility to include explicit $\Delta(1232)$ degrees

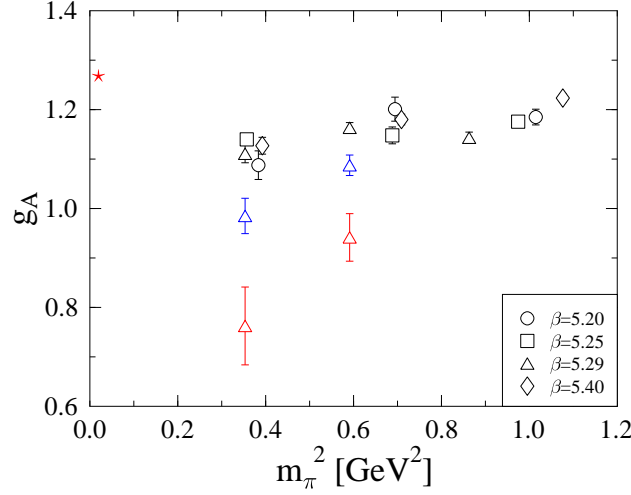


Figure 1: Results for g_A . The red triangles correspond to a spatial box length $L \approx 1.0$ fm, the blue triangles belong to $L \approx 1.3$ fm, and for the black symbols the volumes are larger. The red star represents the physical point.

of freedom in ChEFT. The small expansion parameter in the SSE is called ε , and in $O(\varepsilon^3)$ the mass dependence of g_A is given for infinite volume by [6]

$$\begin{aligned}
g_A^{SSE}(m_\pi^2) = & g_A^0 + \left[4C^{HB}(\lambda) - \frac{(g_A^0)^3}{16\pi^2 F_\pi^2} - \frac{25c_A^2 g_1}{324\pi^2 F_\pi^2} + \frac{19c_A^2 g_A^0}{108\pi^2 F_\pi^2} \right] m_\pi^2 \\
& - \frac{m_\pi^2}{4\pi^2 F_\pi^2} \left[(g_A^0)^3 + \frac{1}{2} g_A^0 \right] \ln \frac{m_\pi}{\lambda} + \frac{4c_A^2 g_A^0}{27\pi \Delta_0 F_\pi^2} m_\pi^3 \\
& + [25c_A^2 g_1 \Delta_0^2 - 57c_A^2 g_A^0 \Delta_0^2 - 24c_A^2 g_A^0 m_\pi^2] \frac{\sqrt{m_\pi^2 - \Delta_0^2}}{81\pi^2 F_\pi^2 \Delta_0} \arccos \frac{\Delta_0}{m_\pi} \\
& + \frac{25c_A^2 g_1 (2\Delta_0^2 - m_\pi^2)}{162\pi^2 F_\pi^2} \ln \frac{2\Delta_0}{m_\pi} + \frac{c_A^2 g_A^0 (3m_\pi^2 - 38\Delta_0^2)}{54\pi^2 F_\pi^2} \ln \frac{2\Delta_0}{m_\pi} + O(\varepsilon^4),
\end{aligned} \tag{4}$$

where g_A^0 denotes the chiral limit value of g_A . This expression depends on several coupling constants, all referring to the chiral limit: F_π is the pion decay constant with the physical value of about 92.4 MeV, Δ_0 denotes the real part of the $N\Delta$ mass splitting, c_A and g_1 are $N\Delta$ and $\Delta\Delta$ axial coupling constants, respectively. Finally, $C^{HB}(\lambda)$ is a counterterm at the renormalisation scale λ , which can be expressed in terms of the more conventional heavy-baryon couplings $B_9^r(\lambda)$ and $B_{20}^r(\lambda)$:

$$C^{HB}(\lambda) = B_9^r(\lambda) - 2g_A^0 B_{20}^r(\lambda). \tag{5}$$

Evaluating the underlying ChEFT in a finite spatial volume yields an expression for the L dependence of g_A [7, 8].

Phenomenology provides some information on the parameters appearing above. The analysis of (inelastic) πN scattering, in particular the process $\pi N \rightarrow \pi\pi N$, suggests that choosing the physical pion mass as the scale λ one has [6]

$$B_9^r(\lambda = m_\pi^{\text{phys}}) = (-1.4 \pm 1.2) \text{ GeV}^{-2}, \quad B_{20}^r(\lambda = m_\pi^{\text{phys}}) \equiv 0. \tag{6}$$

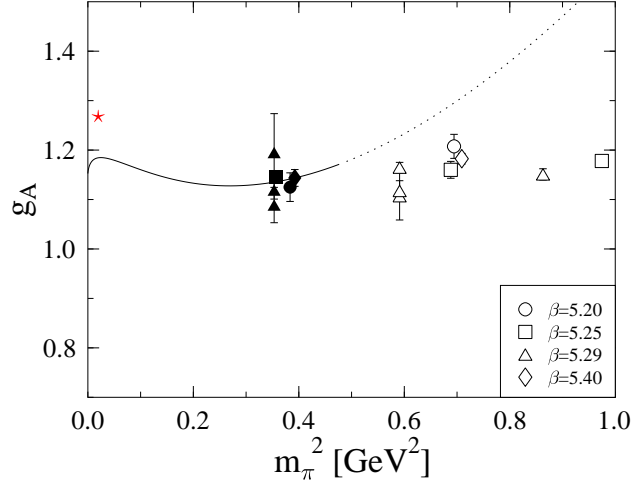


Figure 2: Results for g_A with the finite size correction subtracted. The curve represents the first fit described in the text. The data points shown as open symbols have not been fitted.

Therefore we set $\lambda = 0.14 \text{ GeV}$ in the following and identify $C^{HB}(\lambda = m_\pi^{\text{phys}}) = B_9^r(\lambda = m_\pi^{\text{phys}})$. In the real world one has $\Delta_0 = 0.2711 \text{ GeV}$, and from an $O(\epsilon^3)$ SSE analysis of the Δ width one finds $c_A = 1.5$. At the physical pion mass we have $g_A = 1.267$, while $g_A^0 \approx 1.2$ [6]. Little is known about g_1 . In the SU(6) quark model one finds $g_1 = \frac{9}{5}g_A^0 \approx \frac{9}{5}1.2 = 2.16$. For F_π one expects in the chiral limit $F_\pi \approx 86.2 \text{ MeV}$.

Unfortunately, we cannot fit all parameters. So we fix $\Delta_0 = 0.2711 \text{ GeV}$, $c_A = 1.5$, $F_\pi = 86.2 \text{ MeV}$ and fit g_A^0 , B_9^r , g_1 taking into account only pion masses below approximately 600 MeV. In contrast to Ref. [6] the physical point is not fitted. We find $g_A^0 = 1.15(12)$, $B_9^r = -0.71(18) \text{ GeV}^{-2}$, $g_1 = 2.6(8)$ with $\chi^2/\text{dof} = 4.23/3$. Remarkably enough, these values are very well compatible with our phenomenological prejudices above. In Fig. 2 we plot the data with the finite size correction subtracted together with the fit curve. So, if the fit would be perfect the data points which differ only in the volume would collapse onto a single point.

The uncertainty in g_A^0 is large enough to cover the experimental point. To exemplify this circumstance we fix $g_A^0 = 1.225$, a value well within the range favoured by the above fit, and use only B_9^r and g_1 as fit parameters. We find $B_9^r = -0.66(17) \text{ GeV}^{-2}$ and $g_1 = 3.0(3)$ with $\chi^2/\text{dof} = 4.61/4$. In Fig. 3 we plot the data without subtracting the finite size corrections. Using the results of the last fit we show curves not only for $L = \infty$, but also for the values taken in the simulations for $\beta = 5.29$, $\kappa_{\text{sea}} = 0.1359$. Of course, many more variations of the fit procedure are possible, but the overall pattern remains remarkably stable yielding $g_A^0 \sim 1.2$, $B_9^r \sim -0.5 \dots -0.7 \text{ GeV}^{-2}$, $g_1 \sim 3$ and $F_\pi \sim 90 \text{ MeV}$, in accordance with phenomenological expectations.

Acknowledgements

The numerical calculations have been performed on the Hitachi SR8000 at LRZ (Munich), on the Cray T3E at EPCC (Edinburgh) [9], and on the APEmille at NIC/DESY (Zeuthen). This work

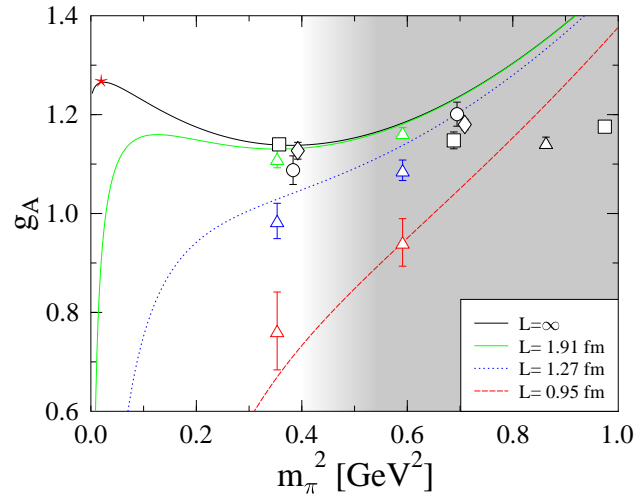


Figure 3: Results for g_A with curves for several values of L .

is supported in part by the DFG (Forschergruppe Gitter-Hadronen-Phänomenologie) and by the EU Integrated Infrastructure Initiative Hadron Physics under contract number RII3-CT-2004-506078.

References

- [1] G. Martinelli, C. Pittori, C. T. Sachrajda, M. Testa and A. Vladikas, *A General method for nonperturbative renormalization of lattice operators*, *Nucl. Phys.* **B445** (1995) 81 [hep-lat/9411010].
- [2] M. Gökeler *et al.*, *Nonperturbative renormalisation of composite operators in lattice QCD*, *Nucl. Phys.* **B544** (1999) 699 [hep-lat/9807044].
- [3] M. Della Morte, R. Hoffmann, F. Knechtli, R. Sommer and U. Wolff, *Non-perturbative renormalization of the axial current with dynamical Wilson fermions*, *JHEP* **0507** (2005) 007 [hep-lat/0505026].
- [4] S. Sasaki, K. Orginos, S. Ohta and T. Blum, *Nucleon axial charge from quenched lattice QCD with domain wall fermions*, *Phys. Rev.* **D68** (2003) 054509 [hep-lat/0306007].
- [5] T. R. Hemmert, B. R. Holstein and J. Kambor, *Heavy baryon chiral perturbation theory with light deltas*, *J. Phys.* **G24** (1998) 1831 [hep-ph/9712496].
- [6] T. R. Hemmert, M. Procura and W. Weise, *Quark mass dependence of the nucleon axial-vector coupling constant*, *Phys. Rev.* **D68** (2003) 075009 [hep-lat/0303002].
- [7] S. R. Beane and M. J. Savage, *Baryon axial charge in a finite volume*, *Phys. Rev.* **D70** (2004) 074029 [hep-ph/0404131].
- [8] T. Wollenweber, Diploma Thesis, Technische Universität München (2005).
- [9] C. R. Allton *et al.* [UKQCD Collaboration], *Effects of non-perturbatively improved dynamical fermions in QCD at fixed lattice spacing*, *Phys. Rev.* **D65** (2002) 054502 [hep-lat/0107021].